REALTIME LINE PARAMETER ESTIMATION USING
SYNCHROPHASOR MEASUREMENTS AND IMPACT OF SAMPLING
RATES

A Thesis by

Anton C. Sameepa Hettiarachchige Don

Bachelor of Science, Southeast Missouri State University, 2014

Submitted to the Department of Electrical Engineering and Computer Science
and the faculty of the Graduate School of
Wichita State University
in partial fulfillment of
the requirements for the degree of
Master of Science

May 2016

REALTIME LINE PARAMETER ESTIMATION USING SYNCHROPHASOR
MEASURMENTS AND IMPACT OF SAMPLEING RATES

The following faculty members have examined the final copy of this thesis for form and content,
and recommend that it be accepted in partial fulfillment of the requirement for
the degree of Master of Science, with a major in Electrical Engineering.

_____
Visvakumar Aravinthan, Committee Chair

_____
M. Edwin Sawan, Committee Member

_____
Ward Jewell, Committee Member

_____
Ehsan Salari, Committee Member

DEDICATION

To my parents for their continuous love, encouragement and support. Also for the absolute thrust placed upon me. I hope to have done you proud.

ACKNOWLEDGMENTS

I would like to express my sincere gratitude and heartfelt appreciation for my advisor, Dr. Visvakumar Aravinthan for all the guidance, support and encouragement throughout the entire graduate process. Over the 2 years I have worked with him, he has become a great mentor, not just academically but also personally. Beyond anything else, Dr. Ara has made me rethink what I believed to be expected of me.

I would like to thank my committee member Dr. Ward Jewell, whose previous study that this thesis is based on, for also providing me with the data and resources in order to accomplish this analysis. His expertise on this area of study was invaluable.

I would like to thank my committee member Dr. Edwin Sawan, who was always there to support me throughout this journey. I would also like to thank him for sharing with me his wisdom and experience, not just in academia, but also in life.

I would like to extend my appreciation towards my committee member Dr. Ehsan Salari for his time, knowledge and for being part of this committee.

I would also like to appreciate the support and guidance given by my dear friends who each in their own capacity have helped me to reach this goal.

Finally, above all else, the deep gratitude I extend towards my parents is beyond words. I am confident that my accomplishment here is a worthy return for all the trust that they placed upon me.

ABSTRACT

The installation of synchrophasor measurement units within the electrical grid system have provided utilities with the ability to monitor their transmission system in real time. These real time observations allow for better situational awareness and rapid responses to adverse system conditions. However, the real time impedance of the powerline is not one of the parameters that is transmitted to the control center and therefore, has to be calculated using the data received from multiple devices. This thesis proposes a simplified methodology for this analysis that requires lower computation power in comparison to most other proposed estimation techniques.

Hence, this methodology is able to produce accurate results faster and by using a smaller quantity of stored data. Due to these reasons, this methodology can be implemented to provide near real time estimation and reporting of impedance values. For the purposes of this research, only the reactance information will be calculated but a similar approach can be used to obtain resistance information as well. The methodology consists of an algorithm to calculate and estimate the reactance of a line using the reported PMU data. It includes an outlier detection and elimination algorithm as well as a denoising technique that makes use of regularized least square estimation to accurately estimate the reactance over the analysis period.

The methodology proposed is tested using real synchrophasor measurement data from a utility provider. The proposed mythology can easily be adapted and applied for the estimation and calculation of other parameters using PMU data.

TABLE OF CONTENTS

LIST OF TABLES

LIST OF FIGURES

LIST OF ABBREVIATIONS

AC	Alternating Current
ADC	Analog to Digital Convertor
AEP	American Electric Power Service Corporation
BPA	Bonneville Power Administration
CAPE	Computer-Aided Protection Engineering
CCVT	Coupling Capacitor Voltage Transformer
CT	Current Transformer
GB	Giga Byte
GOES	Geostationary Operational Environmental Satellite
GPS	Global Positioning System
HMM	Hidden Markov Modeling
Hz	Hertz
IEEE	Institute of Electrical and Electronics Engineers
NASPI	North American SynchroPhasor Initiative
NERC	North American Electric Reliability Corporation
NYPA	New York Power Authority
PLO	Phase-Locked Oscillator
PMU	Synchrophasor Measurement Unit
PT	Potential Transformer
RLS	Regularized Least Square
RMS	Root Mean Square
SCADA	Supervisory Control And Data Acquisition

SCDR   Symmetrical Component Distance Relay

SGIG   Smart Grid Investment Grant Program

SOC   Second Of Century

TVE   Total Vector Error

UTC   Universal Coordinated Time

CHAPTER 1

INTRODUCTION

The electrical grid system in north America can be considered to be a single enormous machine with millions of individual components that work together in sync, with very little margin of error, at all times, every day the year. This level of commitment requires the existence of a highly reliable system with the capability to instantly react to adverse incidents and take actions to mitigate their effects.

In plain contrast to our communications infrastructure, our grid system has changed very little to adapt with the changing times and technologies. It is often said that while Alexander Graham Bell would be astonished at the advances we have made in communications technology; Nikola Tesla would still feel right at home with our current electrical grid system. However, this is about to change drastically with the nationwide roll out of "Smart Grid" technologies. These technologies vary from modern communication systems and cyber security protocols to managing the increasing prevalence of distributed generations and dynamic loads.

An important area of the Smart Grid implementation is more modern sensing and monitoring capability within the grid. The most important and relevant of these is the introduction of SynchroPhasor Measurement Units (PMU) into the system as a replacement for the aging and inadequate SCADA (Supervisory Control and Data Acquisition) system that is currently in place. PMUs are being installed on transmission systems nationwide to provide faster and more accurate "real time" data that is essential for the operation of the autonomous controls in a Smart Grid system. As detailed in this paper, PMU data can be used for a variety of applications in both protection as well as measurement.

While PMUs are a vast improvement over traditional measurement technologies, their data also requires processing in order to extrapolate additional information as well as for error correction.

1.1   Research Objective

Synchrophasor measurement units are installed in high voltage transmission networks where the real-time monitoring of line reactance is of great importance to an operator. In a particularly important application, accurate reactance estimates can be used in conjunction with temperature data to estimate line sag. More reliable real-time estimations can allow utilities to operate the lines at a higher capacity and with a lower margin for error [1]. However, according to current industry standards, reactance is not one of the parameters measured and reported by a PMU [2]. Thus, a variety of techniques have been proposed in literature in order to obtain this information using a variety of mathematical processes [3, 4, 5]. However, since these techniques often require a large sample space and processor intensive calculations in order to produce the output, the 'real-time' benefit of PMUs is often lost. This paper proposes a novel technique for reactance calculation that is able to provide fast outputs with low intensity processes which would allow for near real-time reactance outputs. The techniques developed are verified and optimized using substantial quantities of real PMU data from a major utility provider in the Midwest. The deviation of the output with varying sample spaces and methodology parameters will be explored.

Finally, the variation of outputs, when different standard PMU reporting rates are used is studied. Lower reporting rates will have a substantial reduction in the bandwidth requirement and this is important as PMU networks usually consists of hundreds of units distributed in remote locations where high bandwidth is an expensive commodity.

1.2   Organization of Contents

Chapter 2 will provide a literature review on the mathematical representation of phasors, the fundamentals of synchrophasor measurement units and will provide an overview of the most prevalent estimation and error correction techniques under consideration along with an exploration of their limitations. These will provide the justification for this study.

Chapter 3 will analyze the data that was used for this study. Next, each step of the proposed methodology will be modeled and analyzed. Examples from the available data will be used to show justification for the modeling. The real time application of this methodology will also be discussed.

Chapter 4 will be the sensitivity analysis where the available data will be used to observe how the results of the process change with the variation of certain parameters in the methodology. The selection of the optimal parameters for this study will be discussed.

Chapter 5 will consist of the simulation of the real time application of the methodology using the PMU data. The outline for the simulation is presented and then the resulting output is provided.

Chapter 6 discusses the simulation output from chapter 5 in detail and will also use example sets of data to show validation for the methodology.

Chapter 7 and 8 will contain, respectively, the conclusion and proposed future work.

CHAPTER 2

LITERATURE REVIEW

2.1 Mathematical Representation of Phasors

In 1893, Charles Proteus Steinmetz published his findings on using complex mathematical techniques to model AC networks for analysis [6]. Using these findings and facilitated by the ever advancing processing power available, researchers developed various techniques for the real time monitoring of transmission lines. In 1983, A. G. Phadke et al. [7] documents the use of microcomputer based Symmetrical Component Distance Relays (SCDR) for the application of real time parameter measurement. Phadke will go on to develop the first prototype for a modern PMU system over the next decade. More information on this is given in the next section.

The mathematical representation of an AC waveform in time domain can be in the form of the equation below.

$$x(t) = X_m \cos(\omega t + \theta) \tag{2.1}$$

Where X_m is the magnitude of the sinusoidal waveform and θ is the angular reference of the waveform. ω is from the equation $\omega = 2 \times \pi \times f$, where f is the instantaneous frequency. In phasor form, this equation would be represented as in (2.2) or, if the value is in RMS, as in (2.3) [8].

$$\bar{X} = X_m \angle \theta \tag{2.2}$$

$$\bar{X}_{rms} = \frac{X_m}{\sqrt{2}} \angle \theta \tag{2.3}$$

The correlation between the domains of equation (2.1) and (2.2) can be represented as shown in Figure 1. Plot (a) shows the function in time domain while plot (b) graphs the function as a phasor.
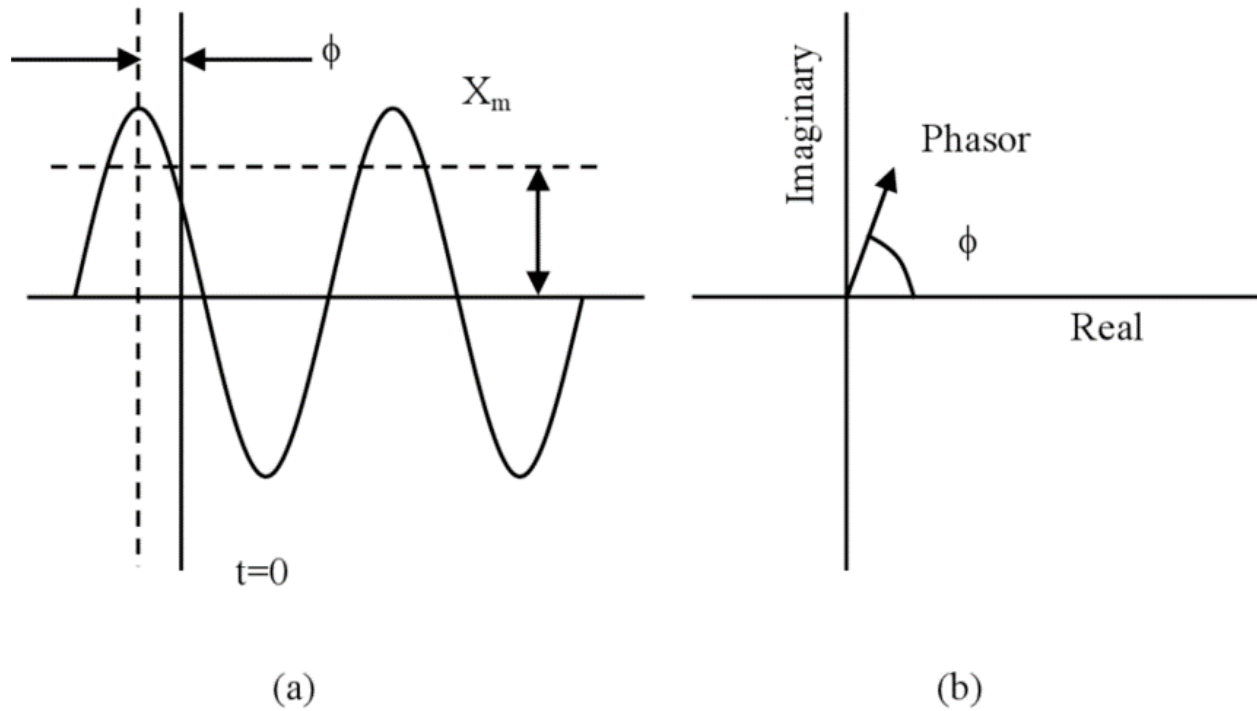
Figure 1. Correlation between time domain and a phasor representation [8]

2.2   Development of Synchrophasor Measurement Units

The IEEE Standard for Synchrophasor Data Transfer for Power Systems (IEEE Std. C37.118.2.2011) governs the fundamental specifications related to synchrophasor measurement units. This section will borrow from this standard as well as some other sources in order to provide the essential basics regarding PMUs.

As previously mentioned, the development of the first modern PMU system was spearheaded by Phadke and his group of researchers at the Power Systems Research Laboratory at Virginia Tech in the 1980s. The concept was based on years of mathematical methods as well as phase angle measurement techniques proposed in recent publications including [9, 10, 11]. The major obstacle at the time was the synchronization of the clocks. [9] and [10] used a radio time signal to synchronize its units while [11] proposed the use of the GOES satellite system that

transmits a signal at a fixed rate of 30 pulses per second. None of these systems provided the accuracy required for the technology to be practical. Phadke used the GPS (Global Positioning System) satellites that were coming online at this time for its time synchronization. This proved to have the accuracy as well as the coverage required.

These early prototype PMUs were installed at some substations under the authority of Bonneville Power Administration (BPA), American Electric Power Service Corporation (AEP) and New York Power Authority (NYPA). A collaboration between Macrodyne Inc. and Virginia Tech produced the first commercial PMU in 1991 [8]. With many other manufacturers quickly showing interest in this product, that same year, the IEEE published its first interoperability standard governing the operation of PMUs and the specifications for their data reporting. The standard undergoes revisions in 2005 and 2011 and currently stands as the *IEEE Standard for Synchrophasor Data Transfer for Power Systems* (IEEE Std C37.118.2-2011). The IEEE standard [2] defines a PMU as:

> *"A device that produces Synchronized Phasor, Frequency, and Rate of Change of Frequency*
> *estimates from voltage and/or current signals and a time synchronizing signal"*

With the United States Department of Energy investing over $65 million in the installation of PMU systems nationwide through the Smart Grid Investment Grant Program (SGIG) and other such investments, utilities are increasing their use of these devices on the grid. Although the median price of a PMU is at $43,400 at the time of this reporting, over 820 devices have been installed through this program as of March 2013 [12]. Figure 2, Courtesy of the North American SynchroPhasor Initiative and the U.S. Department of Energy, show the adoption of PMUs throughout North America as of March 2015.
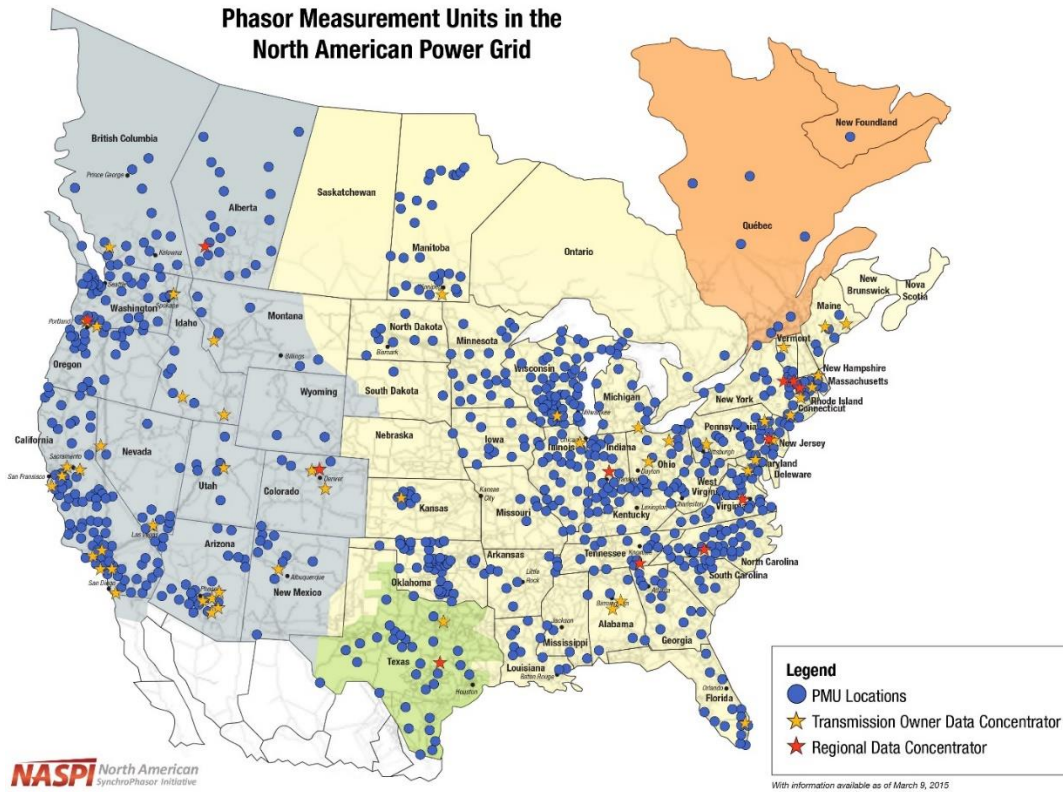
Figure 2. Adoption of PMUs in North America as of March 2015

PMU systems have proven to be invaluable in providing control centers with good situational awareness and decision support. Also, the fast response rates of PMUs mean that they are also used in protection applications such as in [13] and in recent times to aid in smart fault location operations as in [14].

2.3   Operation of Synchrophasor Measurement Units

The PMU itself does not measure the transmission line parameters. It is implemented in conjunction with a set of other devices that feed data into it [15]. These include:

- Potential Transformer (PT) or Coupling Capacitor Voltage Transformer (CCVT) for voltage data.

- Current Transformer (CT) for current data.

- GPS receiver for time synchronization.

- Analog to Digital Convertors (ADC). These are often built-it.

- Communications modem.

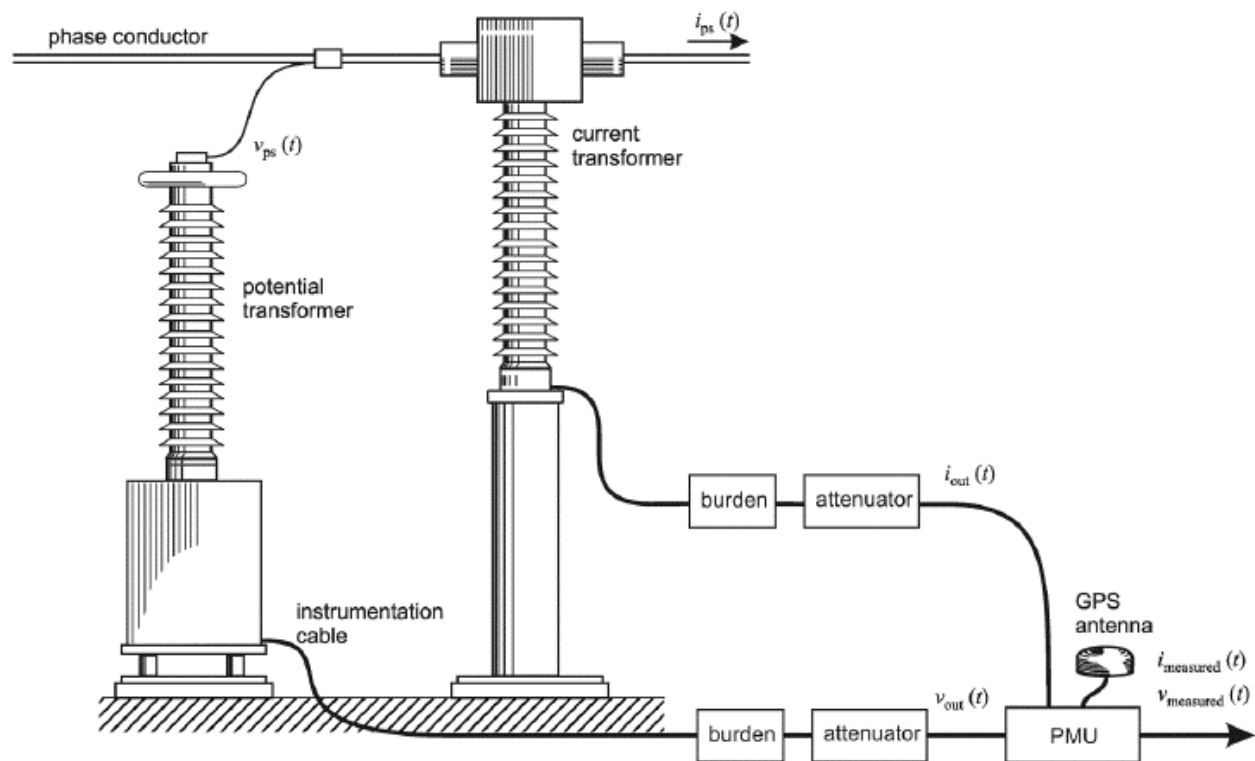The setup can be visualized as shown in Figure 3.

Figure 3. Setup of a PMU system [15]

The time synchronization is achieved with the use of a GPS receiver. This receiver intercepts the Universal Coordinated Time (UTC) broadcasted by the "visible" GPS satellites. The time signal broadcast by GPS is accurate to 2 microseconds and is received every second. A Phase-Locked Oscillator (PLO) then generates the time tags that correspond to the reporting rate of the PMU. However, the time tag reported in not in UTC. Rather, the Second of Century (SOC) format is used. The SOC time is the number of seconds passed since midnight (00:00) of January 1st of 1970. The synchronized time tag consists of 8 bytes during reporting. The first 4 bytes contain the SOC while the next 3 contain a count fractions of seconds from the PLO. This frame size can theoretically count with an accuracy of over one 16 millionth of a second. The last byte is a time quality indicator. This total frame size can accommodate SOC values up to the year 2106.

The PMU uses a ADC along with an anti-aliasing filter to generate a digital output. This sampling rate is often higher than the reporting rate of the PMU and this oversampling allows for better accuracy of the output. The reporting rates that PMU manufacturers must adhere to are laid out in the IEEE standard (IEEE Std C37.118.2-2011) and are shown in Table 1.

TABLE 1

IEEE STANDARD FOR PMU REPORTING RATES **[2]**

System Frequency	50 Hz		60 Hz				
Reporting Rates (frames per second)	10	25	10	12	15	20	30

According to the IEEE standard, a PMU must provide data with a *Total Vector Error* (TVE) of less than 1% under conditions of ±5 Hz off the nominal frequency. The TVE (ε) is defined as "the square root of the difference squared between the real and imaginary parts of the theoretical actual phasor and the estimated phasor, ratioed to the magnitude of the theoretical phasor" [16]. This can be given as a percentage as shown in (2.4).

$$\varepsilon = \left[\sqrt{\left(\frac{(X_r(n)-X_r)^2+(X_i(n)-X_i)^2}{(X_r{}^2+X_i{}^2)} \right)} \right] \times \boldsymbol{100} \tag{2.4}$$

Where X_r and X_i are the theoretical actual synchrophasor values and $X_r(n)$ and $X_i(n)$ are the estimated reported synchrophasor values [8]. r and i standing for real and imaginary respectively.

Minor sources of TVE can result from the burdens within the connection between the measurement transformers and the PMU. However, the most significant source of TVE error in the data reported by the PMU is due to the system operating at off-nominal frequencies [8]. For example, if the system frequency is off by 0.2Hz to 59.8Hz, the period of a waveform can increase from 16.666ms to 16.722ms. This will be an increase of over 0.3%. To mitigate these effects, a PMU uses a set of measurement from before and after the reporting time in order to generate an estimated output.

Equations (2.5) and (2.6) below show how the estimated one-cycle phasor output $\hat{X}$ is calculated using an N number of cycles [7].

$$\hat{X} = \frac{\sqrt{2}}{N} \sum_{k=-\frac{N}{2}}^{\frac{N}{2}-1} x\left[\Delta t\left(k + \frac{1}{2}\right)\right] \cdot e^{-j\left(k+\frac{1}{2}\right)\frac{2\pi}{N}} \tag{2.5}$$

$$\Delta t = \frac{1}{N \times f_{nominal}} \tag{2.6}$$

Where, $x\left[\Delta t\left(k + \frac{1}{2}\right)\right]$ is the voltage or current measurement at $t = \Delta t\left(k + \frac{1}{2}\right)$ and $f_{nominal}$ is the system frequency. However, if the frequency at sampling is not equal to the system frequency, equation (2.7) has to be used,

$$x\left[\Delta t\left(k + \frac{1}{2}\right)\right] = \sqrt{2}\boldsymbol{Real}\left[\overline{X} \cdot e^{-j\left(k+\frac{1}{2}\right)\frac{2\pi}{N}\cdot\frac{f}{f_{nominal}}}\right] \tag{2.7}$$

where, f is the actual frequency at the time of sampling and $\overline{X}$ is the actual phasor value. By combination and simplification of the above equations, we can obtain an equation for $\hat{X}$ as shown below.

$$\widehat{X} = A \cdot \overline{X} + B \cdot \overline{X}^* \tag{2.8}$$

Where, $\overline{X}^*$ is the complex conjugate of $\overline{X}$ and,

$$A = \frac{\sin\left[\pi \cdot \left(\frac{f}{f_{nominal}} - 1\right)\right]}{N \cdot \sin\left[\frac{\pi}{N} \cdot \left(\frac{f}{f_{nominal}} - 1\right)\right]} \tag{2.9}$$

$$B = \frac{\sin\left[\pi \cdot \left(\frac{f}{f_{nominal}} - 1\right)\right]}{N \cdot \sin\left[\frac{2\pi}{N} + \frac{\pi}{N} \cdot \left(\frac{f}{f_{nominal}} - 1\right)\right]} \tag{2.10}$$

Therefore, using equations (2.8), (2.9) and (2.10), we can observe that when $f \rightarrow f_{nominal}$, $A \rightarrow 1$ and $B \rightarrow 0$. Thus, the phasor estimate is very close to the real value as $\widehat{X} \rightarrow \overline{X}$. This effect is reversed as the frequency at measurement moves away from the system nominal frequency [8].

According to the standard, a PMU must report phasor estimates for voltage and current as well as local frequency estimates and rate of change of frequency estimates along with a synchronized time tag [2]. Modern PMU devices can report many additional parameters such as circuit breaker and switching statuses. Under standard reporting rates, a single PMU can transmit over 15 GB of data per year.

Apart from the storage bulk, the reporting rate also effects the bandwidth requirements of the communication system. This can be an issue in remote areas without access to a secure high speed communications network. According to a 2010 study by the North American Electric Reliability Corporation (NERC) [17], the bandwidth requirements can increase rapidly with an increase in the number of PMUs in the system as well as based on their reporting rate.

TABLE 2

APPROXIMATE BANDWIDTH (KBPS) REQUIREMENT FOR A PMU NETWORK

Reporting Rates (frames per second)	Number of PMUs			
	2	10	40	100
10	14	55	209	521
15	29	110	418	1043
30	57	220	836	2085

2.4 Phasor Data Estimation Techniques

As detailed earlier, data from a PMU needs to be processed for errors and outliers. This is achieved by some form of estimation technique as have been thoroughly studied in the literature. The basic idea can be derived from earlier publications such as [18] where the concept of state estimation is well defined. However, this was during a time before PMUs were widely available. More recently publications such as [19, 20] explore how the accuracy of these new technologies can be supplemented by the use of state estimation on the outputs. [21] proposes a novel method of using a hybrid estimation system that makes use the limited number of PMUs available to supplement the data from widely available SCADA systems to improve accuracy.

[22], [23] and other similar studies use these ideas to implement a state estimation system that makes use of the PMU network on the Croatian transmission power system. The findings of these papers show that while state estimation can produce accurate outputs by eliminating random noise and outliers, their effectiveness only increase with an increase in the number of successive samples processed. This increases the processing time and introduces delay.
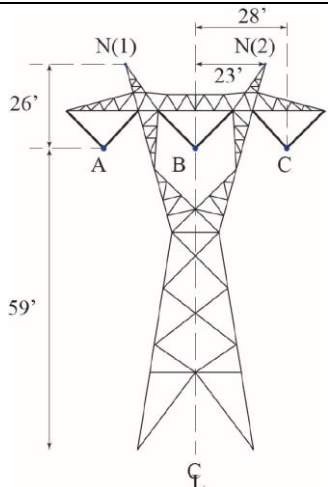
CHAPTER 3

MODELING

An imperative aspect of this research is that all techniques and models proposed have been developed and tested with the use of a real synchrophasor measurement data from a large Mid-Western utility that operates over 200 PMUs across their transmission area.

3.1   Data Selection for Modeling

The analysis was based on 2 PMUs connect across a 20.1 mile transmission line with the following parameters according to the CAPE model developed in [24].

TABLE 3

CAPE MODEL PARAMETERS FOR TRANSMISSION LINE

Parameter	Value
Phase	3 Phase
Nominal Voltage	345 kV
Construction	Homogeneous
Length	20.1 miles
Spans	115
Average Span Lengths	909 feet
Conductors	3 Phases, ACSR Kiwi 2167000 2 Static Neutrals, Alumoweld 7 #8
Tower Construction	

The PMU setup at each end of the transmission line consisted of a CCVT for voltage measurements and a CT for current measurements.

3.2   Analysis of Selected Data

The data consists of a record of 10 parameters from each PMU for a period of 440 days starting from midnight on January 15th 2013 to midnight of March 31th 2014. The reporting rate is 30 frames a second. Theoretically, this would yield a total of over 2.28 billion records for both PMUs. However, in reality the number of records available is significantly less due to a number of reasons including communication errors, GPS synchronization errors, measurement device errors and system down times [22].

A record of data contains the follow.

- *TimeStamp* – Precise GPS time tag.

- *TermID* – Unique Identifier for the PMU

- *CurrentMag* – RMS Current Magnitude

- *CurrentAng* – Phasor Angle for Current

- *VoltageMag* – RMS Voltage Magnitude

- *VoltageAng* – Phasor Angle for Voltage

- *Frequency* – Instantaneous Frequency

- *DFDT* – Rate of Change of Frequency

- *Status* – Circuit Switching Status

- *Digitals* – Digital Relay Information

3.3   Modeling and Analysis of Methodology

Since this study is based on the reactance of the system, the first task was to calculate the instantaneous reactance using the data available.

3.3.1   Calculation of the Reactance

The PMU data contains the time synchronized phasor values (magnitude and angle) for the voltage and current at each end of the transmission line. The absolute single phase voltage output from each PMU for a random 10-minute period is shown in Figure 4. This data set is from data recorded starting at 12 noon on the 15th of January 2013. This data set will be used throughout this methodology discussion.
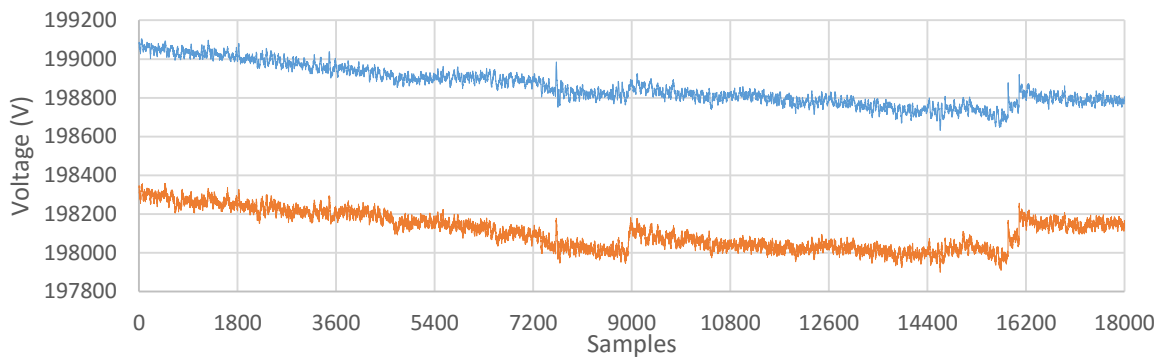

Figure 4. Absolute Single Phase Voltage Output

The absolute single phase current output for a random 10-minute period is shown in Figure 5.
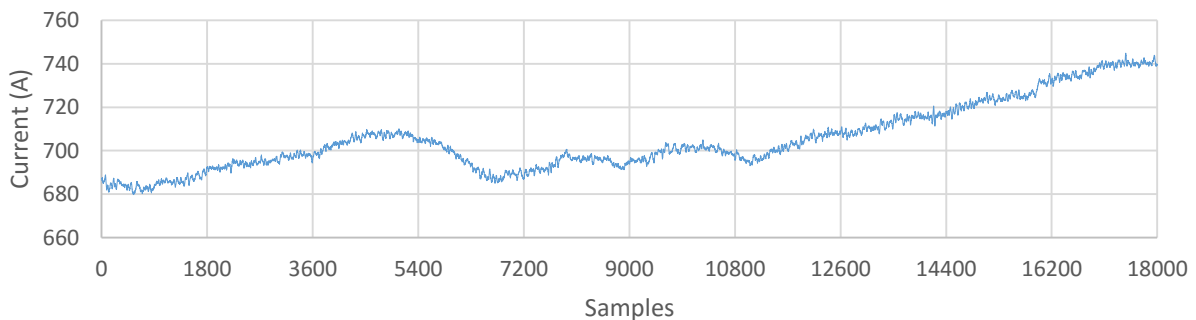

Figure 5. Absolute Single Phase Current Output

15

Using this data, we can calculate the instantaneous reactance at each sample using the equations shown below.

$$V_{1_i} = \left(V_{1mag_i} \times \cos\theta_{v1_i}\right) + j\left(V_{1mag_i} \times \sin\theta_{v1_i}\right) \qquad (3.1)$$

$$V_{2_i} = \left(V_{2mag_i} \times \cos\theta_{v2_i}\right) + j\left(V_{2mag_i} \times \sin\theta_{v2_i}\right) \qquad (3.2)$$

$$\Delta V_i = V_{1_i} - V_{2_i} \qquad (3.3)$$

$$\Delta V_{mag_i} = \sqrt{\left(real(\Delta V_i)\right)^2 + \left(imag(\Delta V_i)\right)^2} \qquad (3.4)$$

$$\theta_{\Delta V_i} = \tan^{-1}\frac{imag(\Delta V_i)}{real(\Delta V_i)} \qquad (3.5)$$

$$Z_i = \frac{\Delta V_{mag_i}}{I_{mag_i}}\angle(\theta_{\Delta V_i} - \theta_{I_i}) \qquad (3.6)$$

Here, V_{1mag_i} and V_{2mag_i} are the voltage phasor magnitudes reported by the 2 devices for the ith sample. θ_{v1_i} and θ_{v2_i} are the voltage phasor angles reported for the same samples. I_{mag_i} and θ_{I_i} are the current phasor magnitude and angle respectively for the ith sample. Z_i is the instantaneous impedance at that sample and therefore the instantaneous reactance can be found as shown below.

$$X_i = imag(Z_i) \qquad (3.7)$$

The resistance and reactance for the above sample of data is shown in Figure 6.
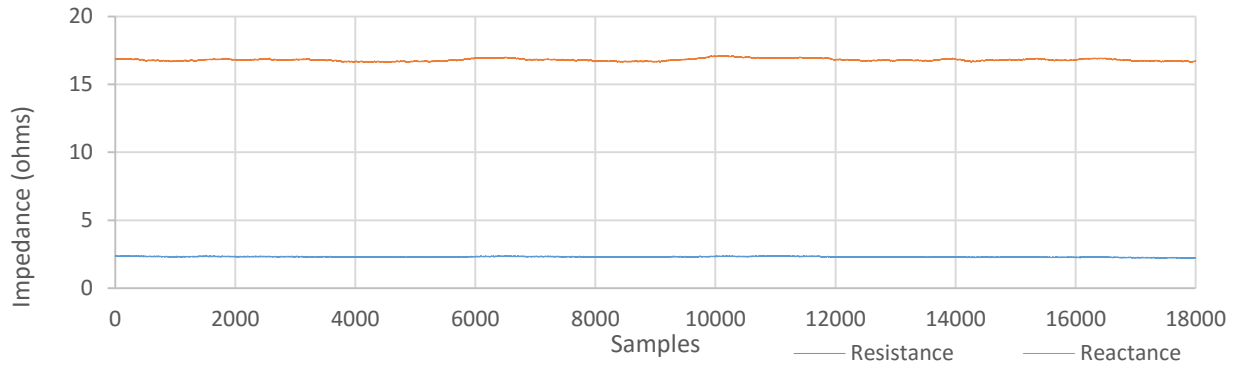

Figure 6. Resistance and Reactance Calculation

3.3.2 Analysis of Reactance

On the figure above, the reactance can be seen to be quite constant. However, upon closer inspection as in Figure 7, we can see that there exists a large amount of noise and variation.
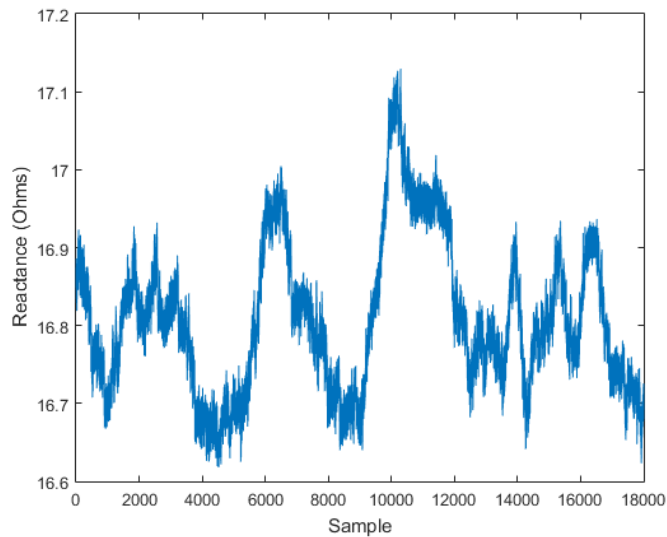

Figure 7. Plot of Reactance

By plotting this data on a histogram as shown in Figure 8, we can obtain its mean as 16.8096 and a sigma as 0.0970.
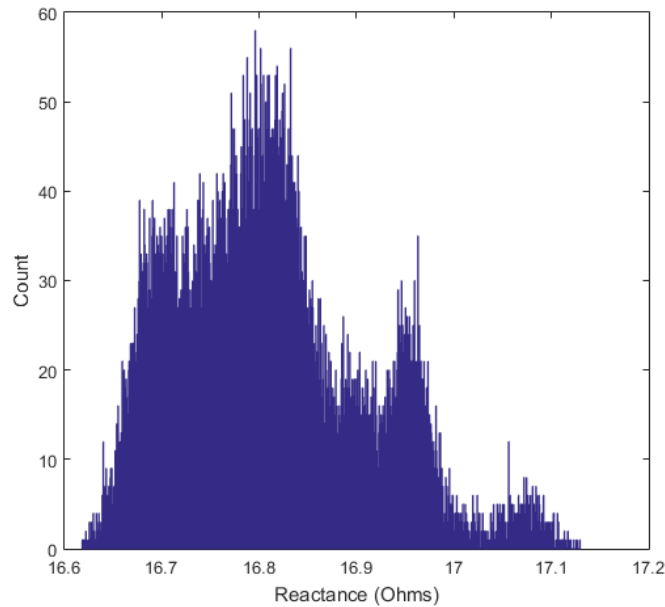

Figure 8. Histogram for Reactance

As can be seen, there exist several peaks on the figure. Upon further analysis, it can be seen that these peaks correlate with variations in frequency as plotted on Figure 9. Farther study is needed regarding this correlation and how it can be used for better estimation. There is more discussion on this in the future work section of the thesis.
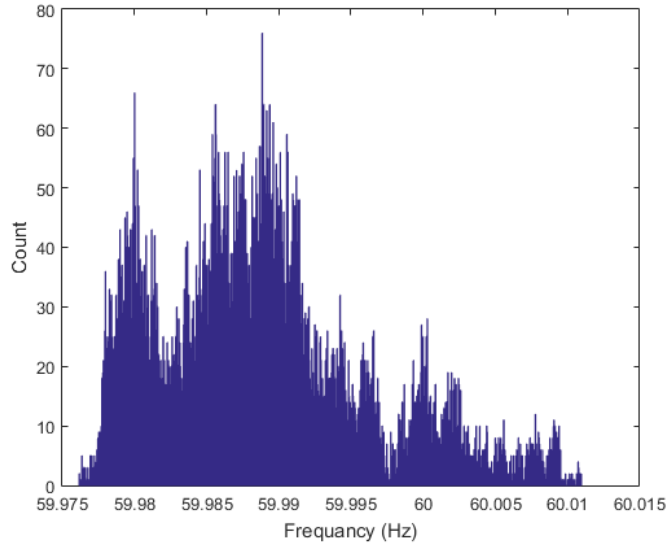
Figure 9. Histogram of Frequency

Now that a data set for reactance has been obtained, the next step in the methodology is to apply an outlier elimination technique. However, in order to make the calculations cleaner, the data will be normalized over the sample period. This step is not essential but is possible as long as the original amplitude values are restored after processing. The normalized representation for the previously selected data is shown in Figure 10.
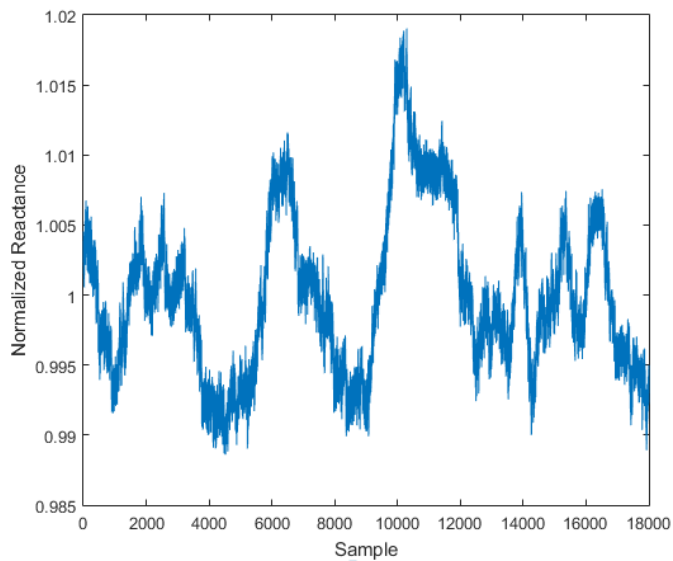

Figure 10. Normalized Reactance Plot

3.3.3 Application of Outlier Elimination Technique

For outlier elimination, 2 techniques were considered and tested. The Grubb test for outliers is a useful method of identifying outliers in an approximately normal distribution. The test finds the maximum point on a dataset and compares its distance from the mean against a preset *critical value* that is determined by the input α. If the point lies outside this limit, it is classified as an outlier. This test is an iterative process that will remove one outlier per cycle until all values are within the limits. However, due to this iterative process, in this implementation with a large number of data points, it can be expensive both in terms of time and processing power.

In contrast, a simple 3 sigma outlier test works well in this setting. It is also more efficient in its execution as it only needs to read through the data set one time. The maximum (X_{max}) and minimum (X_{min}) limits for acceptable data are set by using equations (3.8) and (3.9) respectively.

$$X_{max} = m_{X_{norm}} + 3 \times \sigma_{X_{norm}} \tag{3.8}$$

$$X_{min} = m_{X_{norm}} - 3 \times \sigma_{X_{norm}} \tag{3.9}$$

Where $m_{X_{norm}}$ and $\sigma_{X_{norm}}$ are the mean and sigma values of the normalized reactance dataset X_{norm}.

Using these limits, the data set will be scanned for outliers. When a data point is found to be beyond this limit, the value of this data point is replaced with either the maximum or minimum limit value. While these outlier data points might be important in the application of fault analysis, this study is more focused on obtaining the parameters of the system under normal conditions and therefore these outlier points are removed in order to not skew the overall data reported. However, it is also possible to use a prediction algorithm to deduce more accurate values for these outlier points by analyzing the data around this point. More discussion on this is done in the future work section.

3.3.4 Analysis of Outlier Elimination Technique

Figure 11 shows the output of the above elimination technique when used on the data set under investigation. In comparison to Figure 10, clipping can be seen on the highest points of the dataset where the limits have been exceeded.
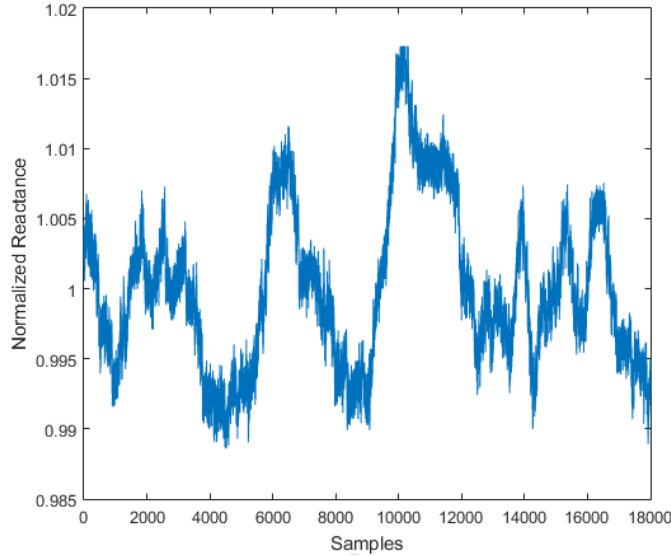

Figure 11. Elimination of Outliers

3.3.5 Application of RLS Denoising

Due to the exactly-determined nature of this estimation, a least squared optimization with x unknown parameters and b measurements as given in (3.10) will not be appropriate.

$$\min\|x - b\|^2 \tag{3.10}$$

To yield a meaningful solution we need to make use of a regularization factor using some previously known nature of the parameter. In the case of this study, we use the a priori assumption that the progression of data is smooth. Therefore, a quadratic penalty is added in the form of the sum of the squares of the difference of the consecutive components in the progression. This penalty factor $R(x)$ can be perceived as below [25].

$$R(x) = \sum_{i=1}^{n-1}(x_i - x_{i+1})^2 \tag{3.11}$$

Where, n is the number of data points.

To get a better understanding, we can write this in a matrix form where, $R(x) = \|Lx\|^2$ with the L matrix of size $(n-1) \times n$.

$$L = \begin{pmatrix} 1 & -1 & 0 & 0 & \cdots & 0 & 0 \\ 0 & 1 & -1 & 0 & \cdots & 0 & 0 \\ 0 & 0 & 1 & -1 & \cdots & 0 & 0 \\ \vdots & \vdots & \vdots & \vdots & \ddots & \vdots & \vdots \\ 0 & 0 & 0 & 0 & \cdots & 1 & -1 \end{pmatrix} \quad (3.12)$$

We can then write a regularized least squares problem and add a regularization parameter λ to govern the denoising effect.

$$\min_{x} \ \|x - b\|^2 + \lambda\|Lx\|^2 \quad (3.13)$$

Hence, the optimal solution to this can be found using the equation below.

$$X_{rls}(\lambda) = (I + L\lambda^T L)^{-1}b \quad (3.14)$$

In the sensitivity analysis chapter of this research, different values of λ have been used to study the effect on the denoising output. From the equations above we can deduce that increasing λ increases the regularization effect and therefore, in this application, will increase the smoothness of the output.

3.3.6 Analysis of RLS Denoising

Using $\lambda = 1000$, the data set under investigation was denoised. The resulting output is shown in Figure 12.
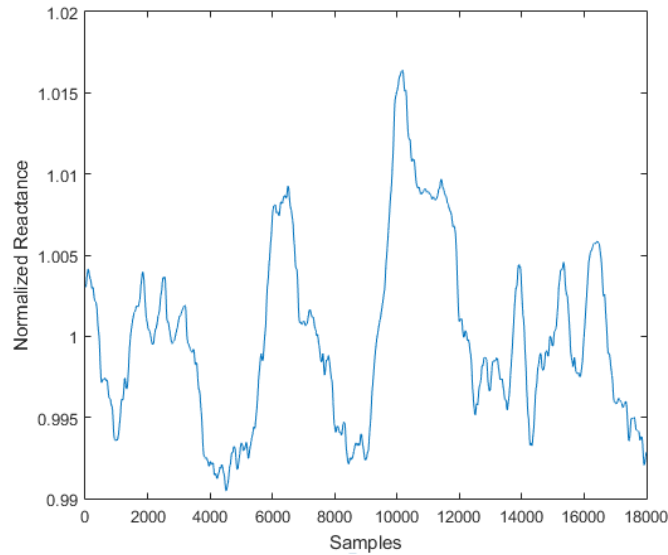

Figure 12. Denoised Normalized Reactance

In comparison with the normalized dataset, the mean value remained constant while the σ changed from 0.0058 to 0.0056.

3.3.7 Reconstruction of Original Amplitude.

Since the above processes were carried out after normalizing the data, we need to reconstruct the dataset by multiplying with its mean. Comparison between the reconstructed data against the original reported data shows the effect of this process. For the data set used here, the mean remained constant while the σ saw a reduction from 0.0970 to 0.0944. The effect of the denoising can be clearly seen in Figure 13.
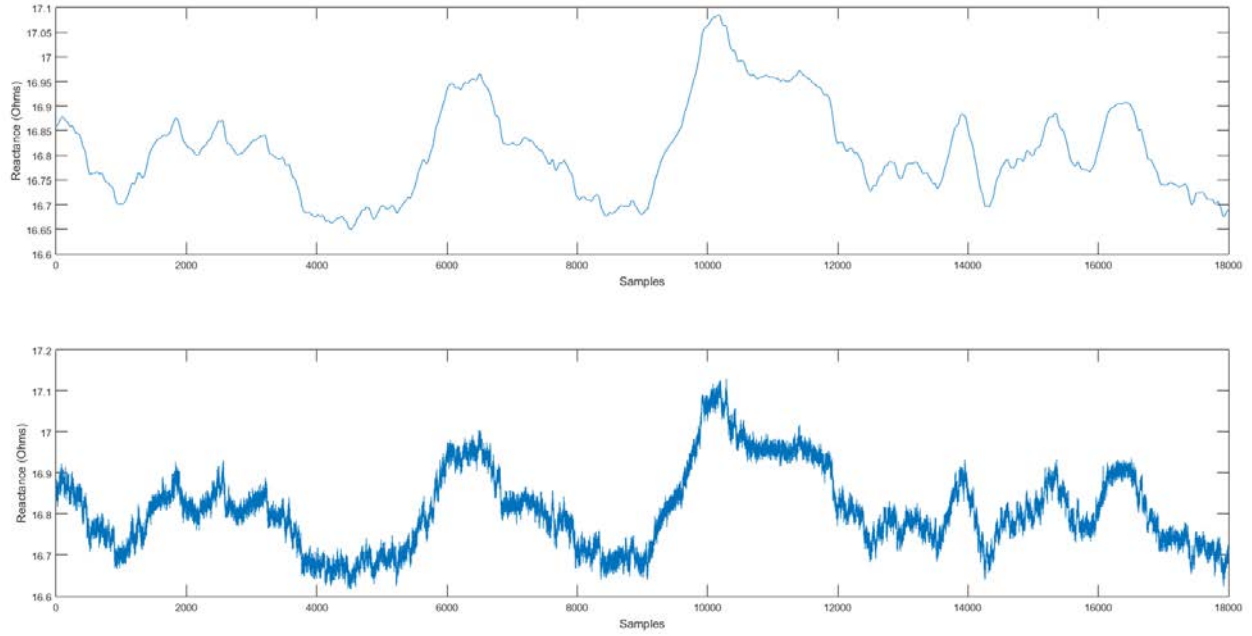
Figure 13. Comparison to Original Data Set

If a smaller dataset is examined, the effect of this process can be seen to be more profound.

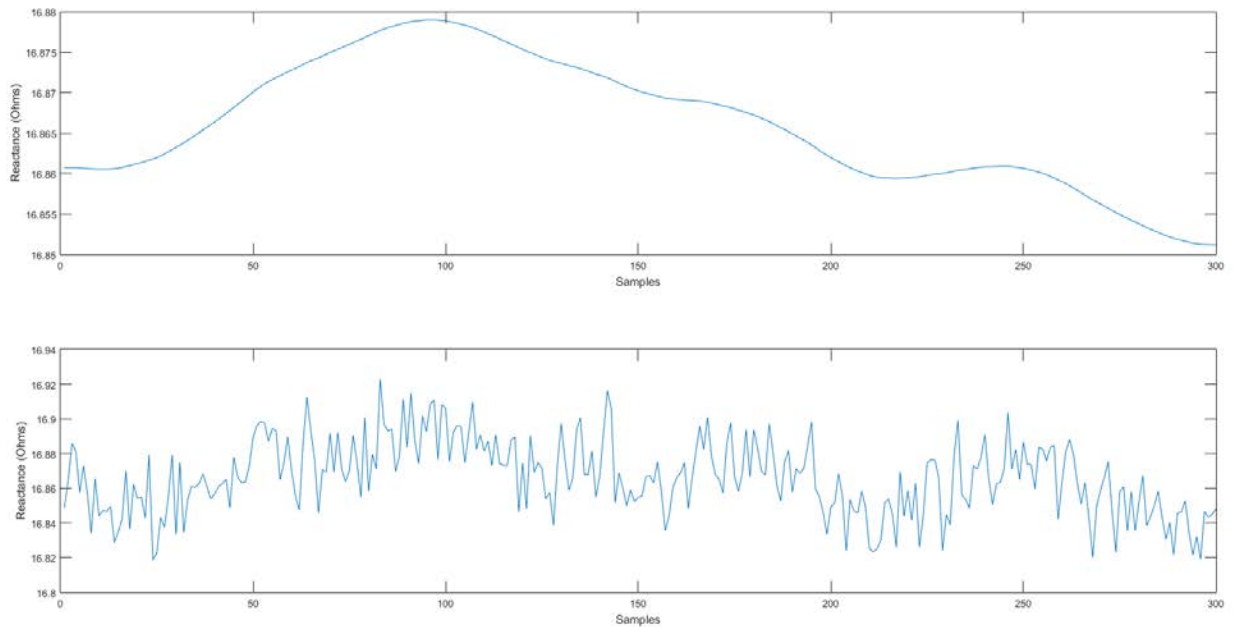For example, a 10 seconds section of the above data can be processed as shown below.

Figure 14. Comparison of Smaller Data Sets

In this comparison, the σ drops from 0.0213 to 0.0078 while the mean remains constant. More analysis of the sensitivity to data period have been done in the later chapters.

3.3.8   Generation of Mean Reactance Values.

After obtaining the reconstructed dataset, the mean of the reactance value is found over the period of analysis. This is the final step of the process to reproduce a denoised and estimated value for reactance. For example, ten minutes of data can be used to produce an output that is processed in 30 second intervals. The result will be a set of data representing an accurate estimate of reactance for each 30 second interval. The outcome of this step is shown in the figure below.
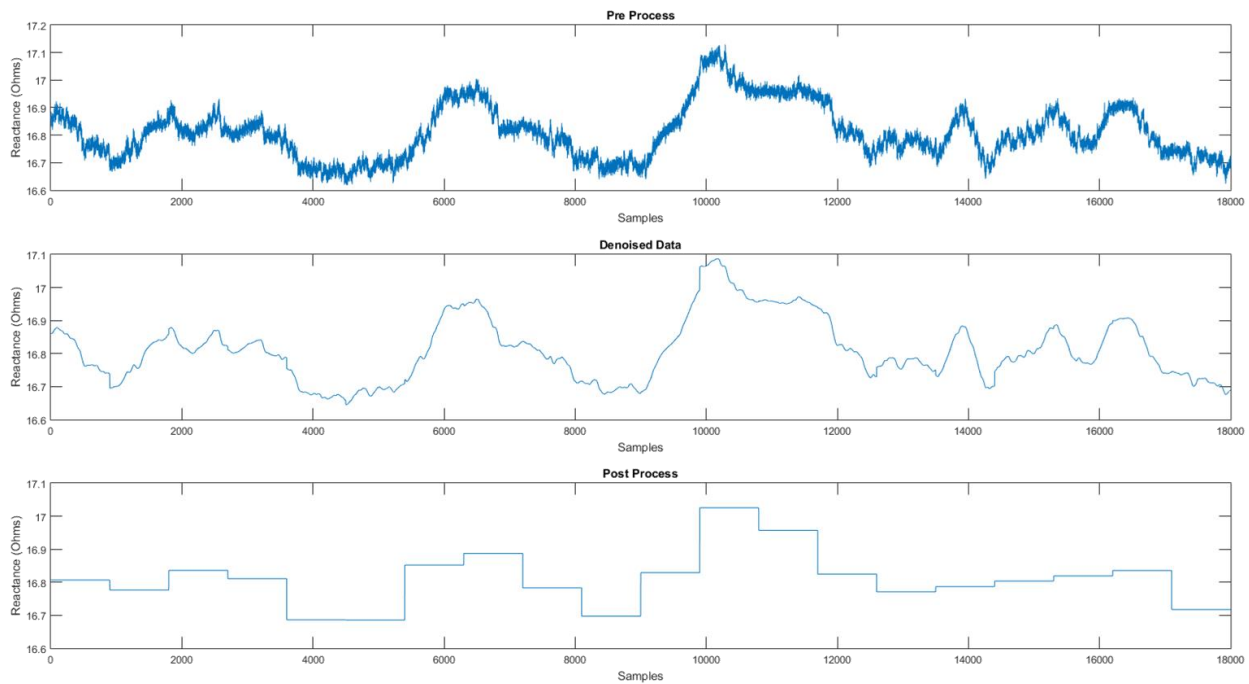

Figure 15. Generation of Mean Reactance Values

3.4 Application in Real Time

The most processer intensive tasks in this methodology are the creation of the regularization matrix and the computation of its optimal solution. However, since we predefine the

basic parameters of the process, namely the regularization factor and the analysis period, this step

can be computed and stored beforehand.

In a real time application, the following steps will be taken to produce the output rapidly.

- Data for the defined analysis period is received from the PMU.

- Date is normalized and the outlier limits defined.

- Data is tested for outliers and such data point are redefined.

- Data is denoised by multiplication with a preloaded regularization matrix.

- Data is reconstructed to its original amplitude.

- The mean of the reconstructed data is produced as the output.

CHAPTER 4

SENSITIVITY TO METHODOLOGY PARAMETERS

The elimination and estimation methodology proposed in this paper has three distinct parameters that can be changed to affect the output. These three parameters, as listed below, will be studied to see the influence each of them have over the output.

- The time period of the analysis is a factor that can influence the output.

- The regularization parameter, λ, in the denoising process can be changed to effect the amount of denoising done on the data.

- Finally, the reporting rates of the PMU can be changed to effect the accuracy of the data.

    Since these factors are independent, for each of the studies below, two of these factor have been held constant while the third is tested with different values. For each test, 50 random data sets from throughout the year have been processed and the following data collected for each of the data sets.

- Average Mean of the Output data

- Average Standard Deviation of the Output data

- Normalized Standard Deviation as a percentage of the average mean

The averages of each of the above values will be used to study how the factor under investigation affects the output of the process.

4.1 Effect of Time Period of Analysis

A valuable outcome of this study would be to produce an accurate output using a smaller sample size. In this section, the variation of the average mean and standard deviation are compared for six different analysis periods. For this set of tests, the λ was set at 1000 and the reporting rate at 30 per second. The outcome is shown in the table below.

TABLE 4

EFFECT OF TIME PERIOD OF ANALYSIS

Period Tested (seconds)	Average Mean	Average Sigma	Normalized Standard Deviation (%)
600	23.22797211	3.038482578	13.081%
300	22.89954918	0.769769551	3.362%
60	23.05835598	0.333845582	1.448%
30	22.93393881	0.318316254	1.388%
10	22.79941963	0.075716108	0.332%
1	22.73097803	0.007016139	0.031%

These values can be plotted as below.
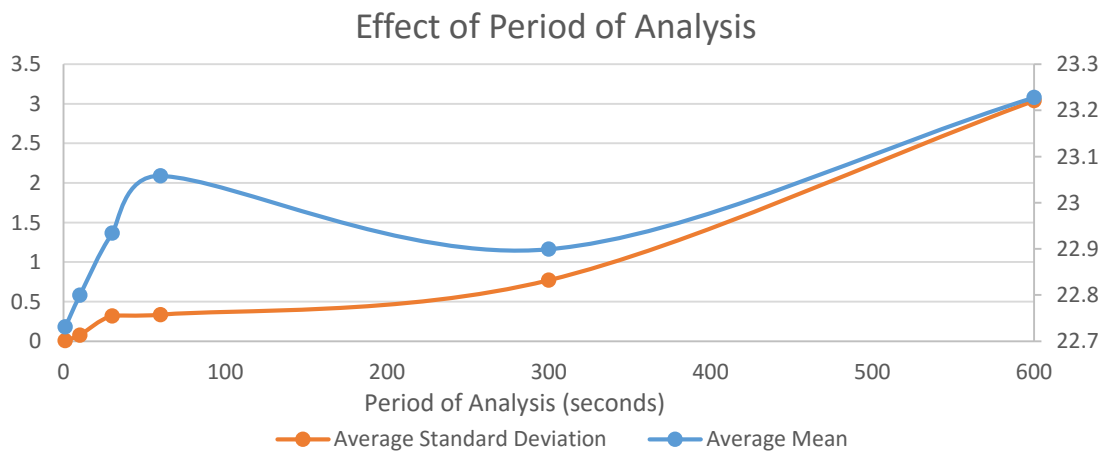

Figure 16. Variation of average mean and standard deviation with changing period of analysis.
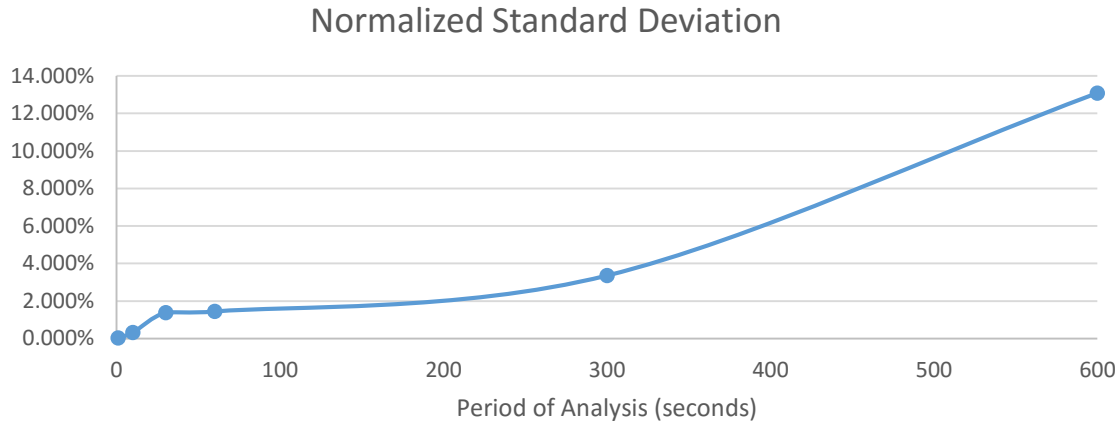
Normalized Standard Deviation

Figure 17. Variation of normalized standard deviation with changing period of analysis.

The data shows that under 30 seconds, the number of samples is too low to produce an accurate estimation and thus there an abrupt drop in the standard deviation. From the 30 second mark onwards, percentage is quite constant until the 300 second mark. After 300 seconds, there is a high deviation from the original sample. Since for this application a lower time period is better, 30 seconds seem to be the optimal low value we can pick to still produce accurate results.

4.2   Effect of Regularization Parameter

As discussed earlier, the denoising effect in the methodology is governed by the regularization parameter, λ. A very small λ will not yield any reasonable denoising and the output will be very similar to the original. A very high λ will yield a very smooth output. However, it will be a very poor estimate of the original. Therefore, a λ must be selected that will strike a compromise between smoothness and accuracy of the output. For these tests, the time period has been kept at 30 seconds and the reporting rate a 30 per second. Three values of λ were tested and their effects are shown in the table below.

TABLE 5

EFFECT OF REGULARIZATION FACTOR

Regularization Parameter (λ)	Average Mean	Average Sigma	Normalized Standard Deviation (%)
1000	23.09425465	0.320112002	1.386%
100	22.54845647	0.391950241	1.738%
10	22.59722953	0.446297138	1.975%

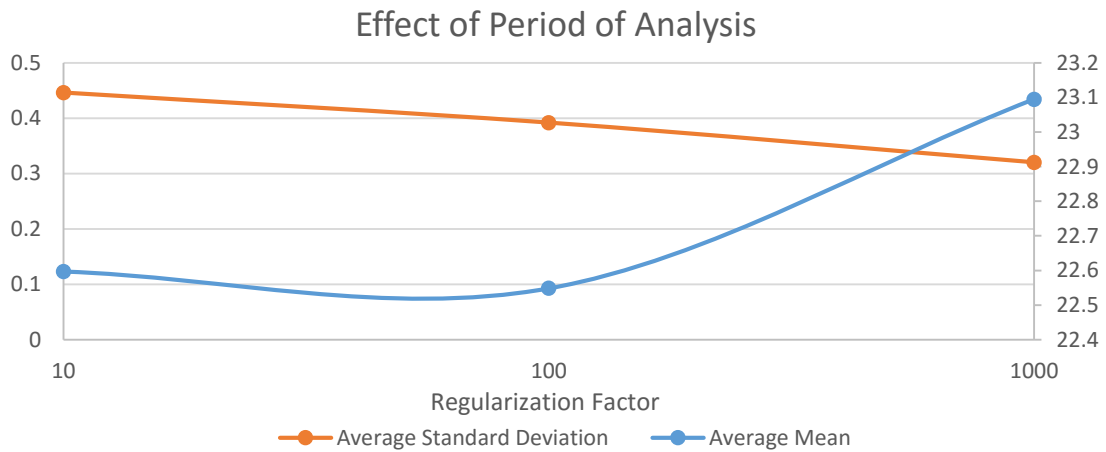These values can be plotted on a logarithmic scale as below.

Figure 18. Variation of average mean and standard deviation with changing regularization factor.
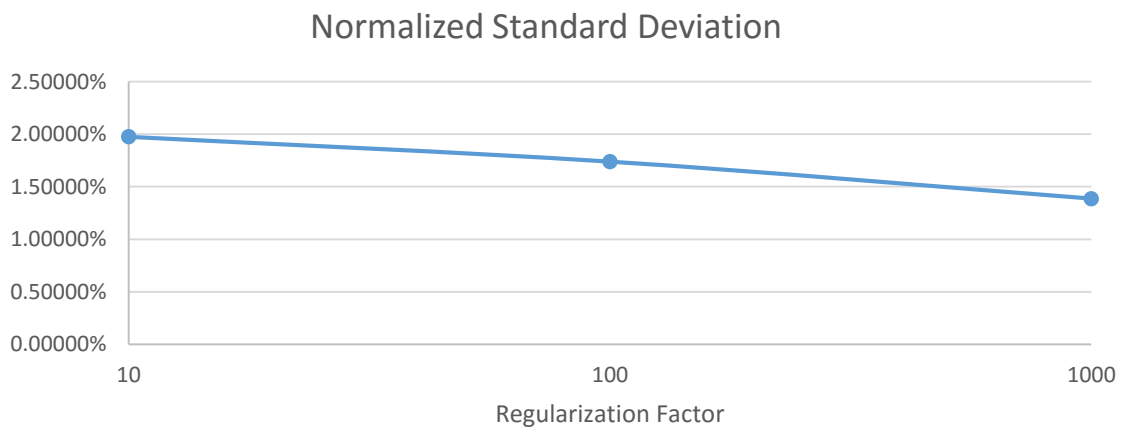

Figure 19. Variation of normalized standard deviation with changing regularization factor.

In the application of denoising, the optimal solution would be one that yields an output that is very close to the mean of the original. However, since we need the output to be minimized in terms of noise, a more important factor would be for the optimal solution to have a low sigma value. Therefore, from the data above, it can be concluded that a λ of a 1000 would result in an accurate representation of the input data with good noise reduction.

For illustrative purposes, the figure below shows a single 30 second period of data with a comparison of the denoising effect with varying regularization factors of 10, 100 and 1000.
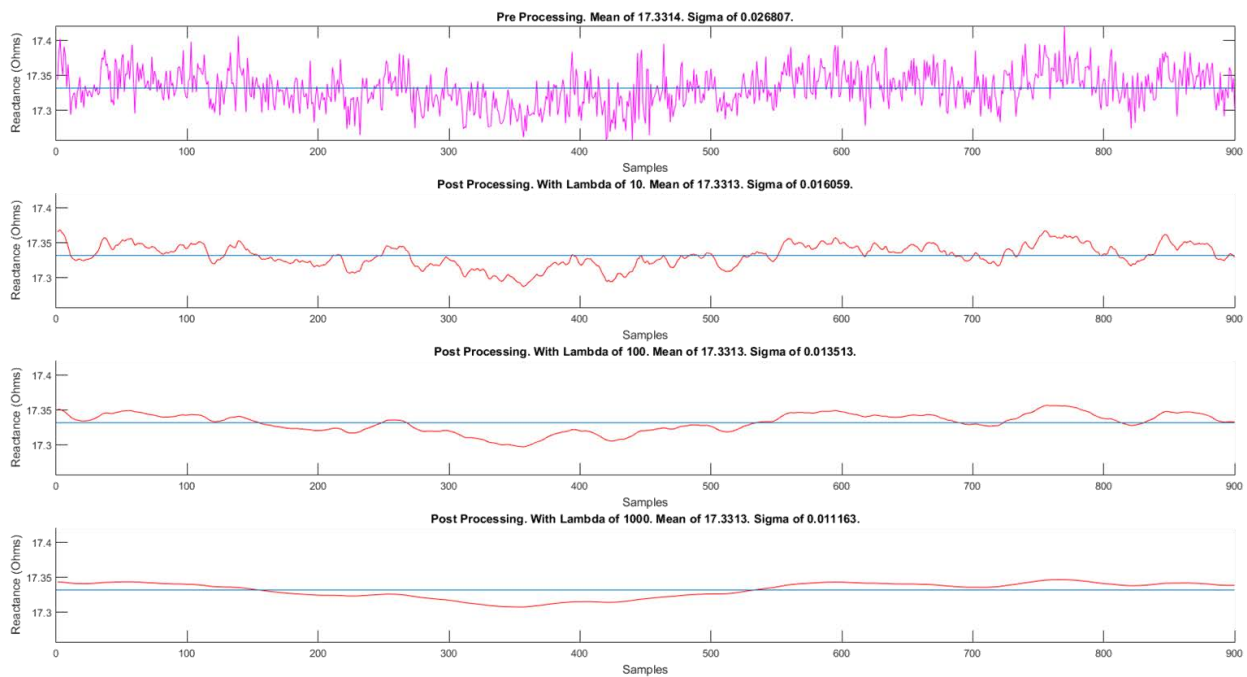

Figure 20. Effect of changing regularization factor.

4.3 Effect of Reporting Rates

According to IEEE std. c37.118, in a 60 Hz system, PMUs can be configured to report at five different time intervals. A low reporting rate will save on communication bandwidth but might hinder an accurate estimation of parameters. However, if a satisfactory level of estimation can be achieved using a lower reporting rate owing to the regularization effect in this methodology, it could mean that a low bandwidth communication system would be viable. For this test, the time

period for analysis was kept at 30 seconds and the regularization factor at $\lambda=1000$. The reporting

rates of 10, 15 and 30 times a second were evaluated to see how the output vary. The findings are

shown in the table below.

TABLE 6

EFFECT OF PMU REPORTING RATE

Reporting Rate (per second)	Average Mean	Average Sigma	Normalized Standard Deviation (%)
30	23.09425465	0.320112002	1.386%
15	22.93371053	0.268807201	1.172%
10	22.93659653	0.224543324	0.979%

These values can be plotted as below.
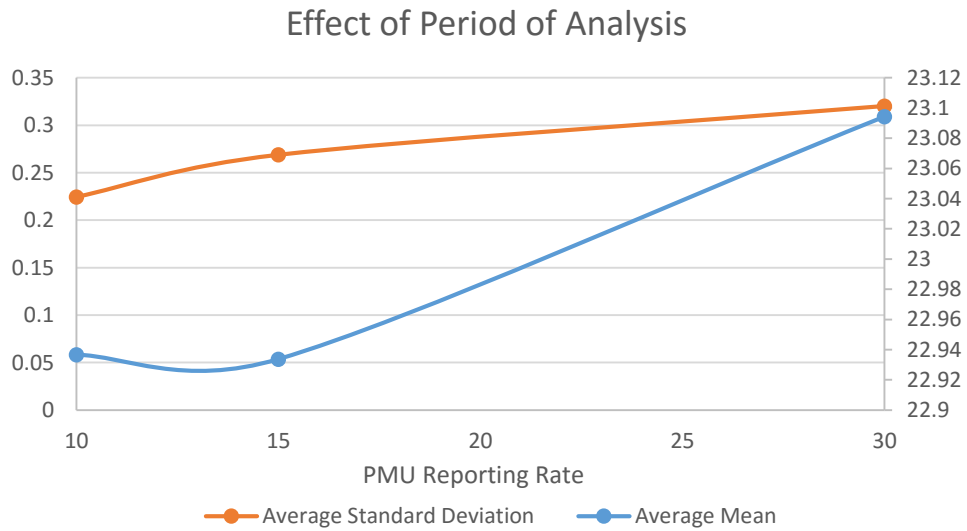
Effect of Period of Analysis

Figure 21. Variation of average mean and standard deviation with changing PMU reporting rate.
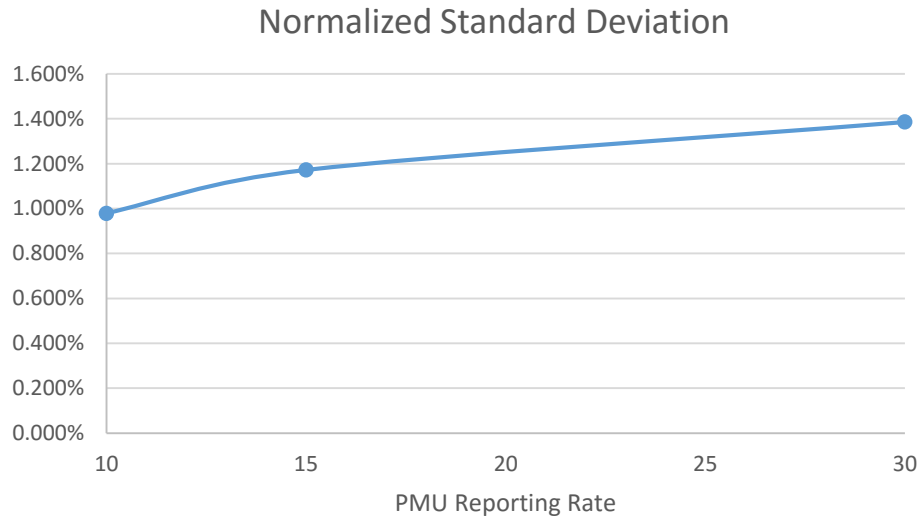
Figure 22. Variation of normalized standard deviation with changing PMU reporting rate

Based on the results above, it can be observed that a reduced reporting rate would result in a lower standard deviation of the output. This is due to the reduced number of data points available for accurate denoising. However, the change is very small and depending on the application, this reduced accuracy might be tolerable in exchange for a lower bandwidth usage.

For illustrative purposes, the figure below shows a single 30 second period of data plotted used reporting rates of 30, 15 and 10.
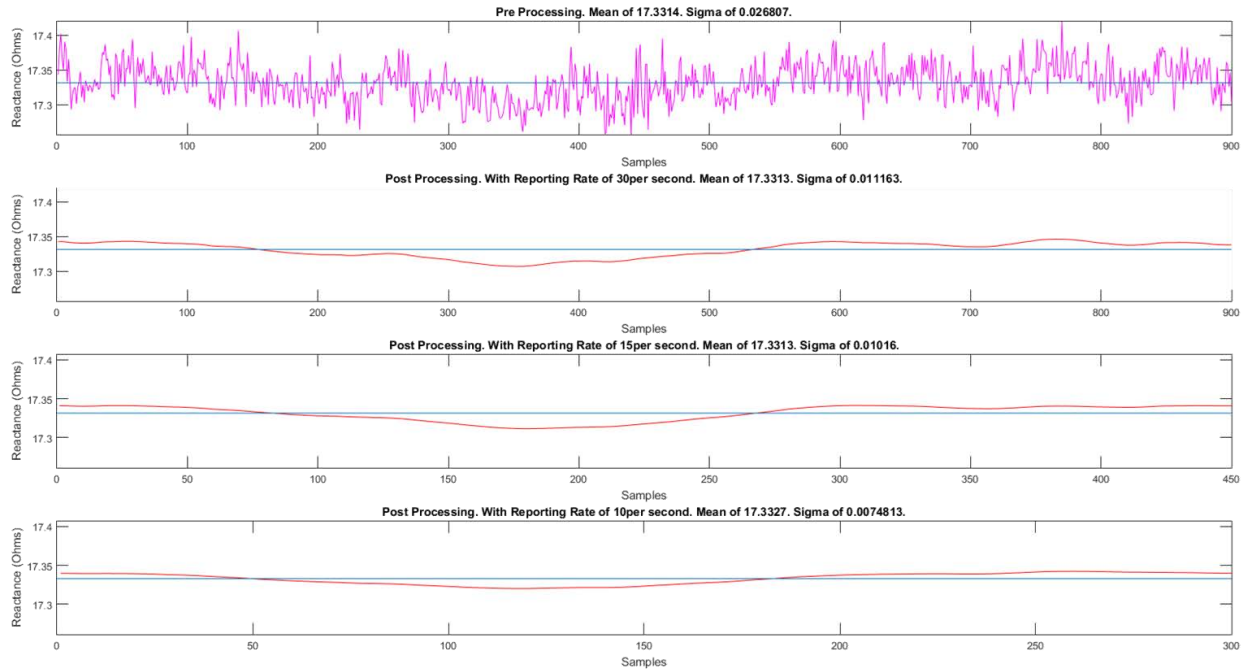
Figure 23. Effect of changing PMU reporting rate

4.4 Effect of Varying Parameter

Using the values calculated throughout this chapter, observations can be made regarding the extent of influence each of the variable parameters have on the outcome of the process.

TABLE 7

EFFECT OF VARYING PARAMETERS

Variable Parameter	Tested Change in Parameter	Change in Outcome Standard Deviation	Influence on output per percent change in parameter
Analysis Period	60000%	42197%	70.33%
Regularization Parameter	10000%	70%	0.70%
Reporting Rate	300%	142%	47.19%

Table 7 shows that the largest influence of the output can be achieved by varying the analysis period and that a change in the PMU reporting rate has a lower impact on the outcome. The regularization parameter has a low impact on the overall change in standard deviation as it applies more on the scale of individual data points. An even larger value of λ would have a larger impact. However, by this point, the output data will lose accuracy.

CHAPTER 5

DATA ANALYSIS AND RESULTS

In this chapter, the proposed methodology was used to analyze a set of data as a simulation of real time processing. The computation consisted of the steps defined in section 3.4 to process and output an accurately estimated and denoised value for reactance.

5.1   Basis for Parameter Selection

As a result of the sensitivity tests done earlier, the following parameters were selected with which to simulate.

- The period of analysis was set to 30 seconds so as to provide a useful quantity of data but without a significant delay in processing.

- The regularization factor λ was set to 1000 so that a sufficient extent of denoising is applied.

- The PMU reporting rate was set to 30 per second so as to produce the best possible estimation.

5.2   Selection of Data for Analysis

In order to run multiple iterations of the analysis under varying conditions, fifty sets of data from random months, days and times were fed to the simulation. Each dataset contained 10 minutes of data that was analyzed in 30 second periods. This is similar to how a real time application would be implemented.

5.3   Results of Analysis

The data collected contained a few outlier records that could have been due to a variety of reasons including equipment failures or actual transmission system faults. After accounting for these outlier records, the average mean and standard deviation for the whole set of data was calculated along with the normalized standard deviation. The results are shown in the table below.

TABLE 8

AVERAGE MEAN AND STANDARD DEVIATION FOR TEST DATA

Average Mean	Average Sigma	Normalized Standard Deviation (%)
23.71936517	0.299281359	1.262%

These results are discussed in detail in the next chapter.

The methodology also shows how the mean reactance would change based on the loading situation of the grid. This can be observed by studying the mean reactance output at various times of the day and at different seasons.

Comparison between Figure 24 and Figure 25 show the change in reactance value between the noon and the afternoon on a summer day due to changes in the system load.
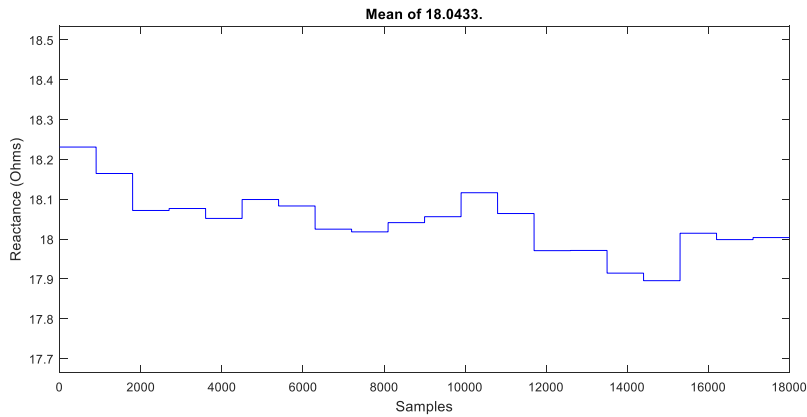

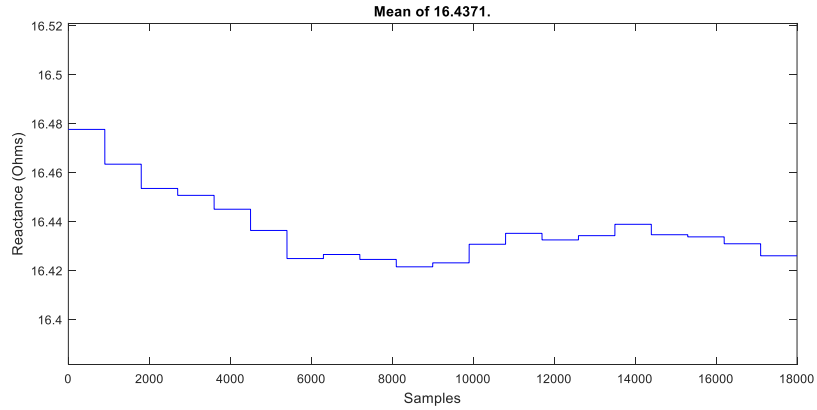Figure 24. Reactance near Noon during the Summer Season.

Figure 25. Reactance around 3 p.m. during the Summer season.

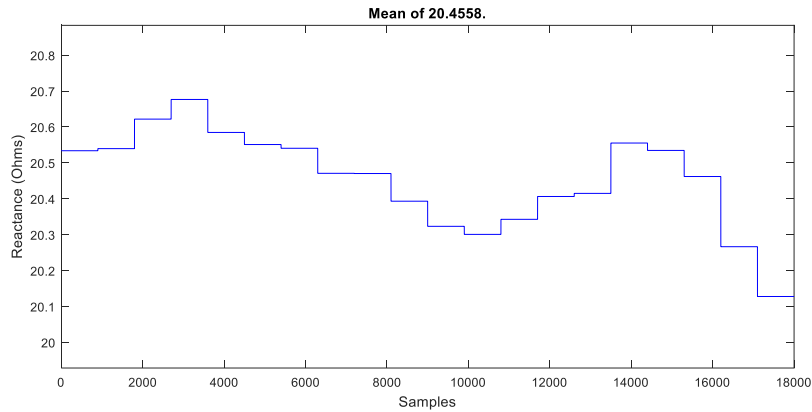Below is a comparison between periods during the late night and late morning on a winter day.

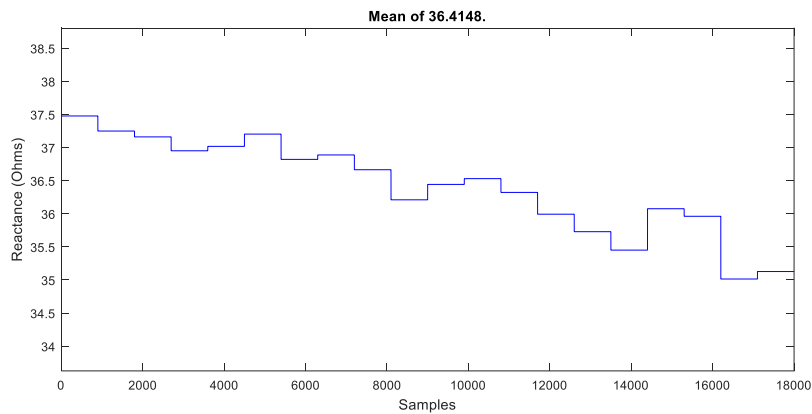Figure 26. Reactance around late Night during the Winter Season

Figure 27. Reactance around late Morning during the Winter Season

CHAPTER 6

DISCUSSION OF RESULTS

The results obtained in the earlier chapter are very close to those observed during the sensitivity analysis testing with identical parameters. This is an indication that the methodology functions well under large amounts of data. Also, it shows that it is possible to get sufficiently accurate data in near real-time.

The simulation also considered a wide verity of seasons and times of the day for analysis. The methodology was able to function well enough to accommodate the dynamic nature of the transmission system during all these instances. Examples of data extracted for such varying conditions are shown below.

In the data extraction below, the change in reactance can be observed for a ten minute section of time starting at around 4 p.m. on the 16th of August 2013.
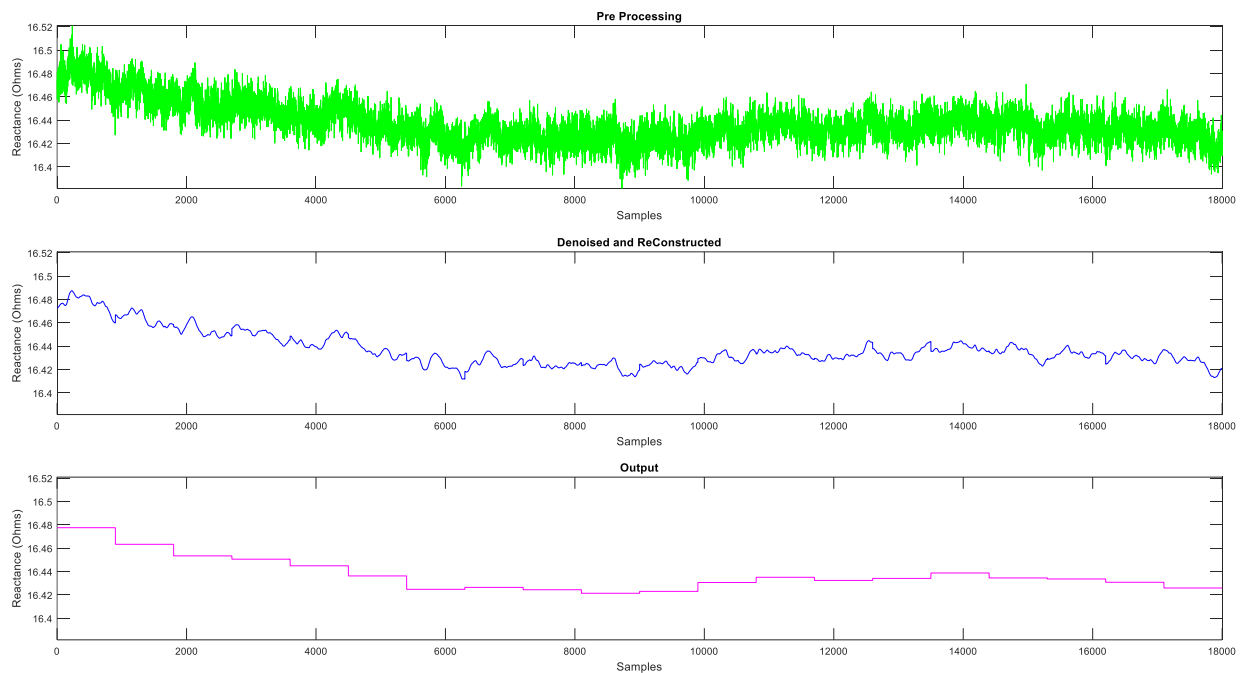
Figure 28. Ten Minute Example 1

In the results, the output can be seen to follow the gradual change in reactance well and at the same time achieve a good reduction in noise.

This next section of data is from around midnight on the 2nd of February 2013.
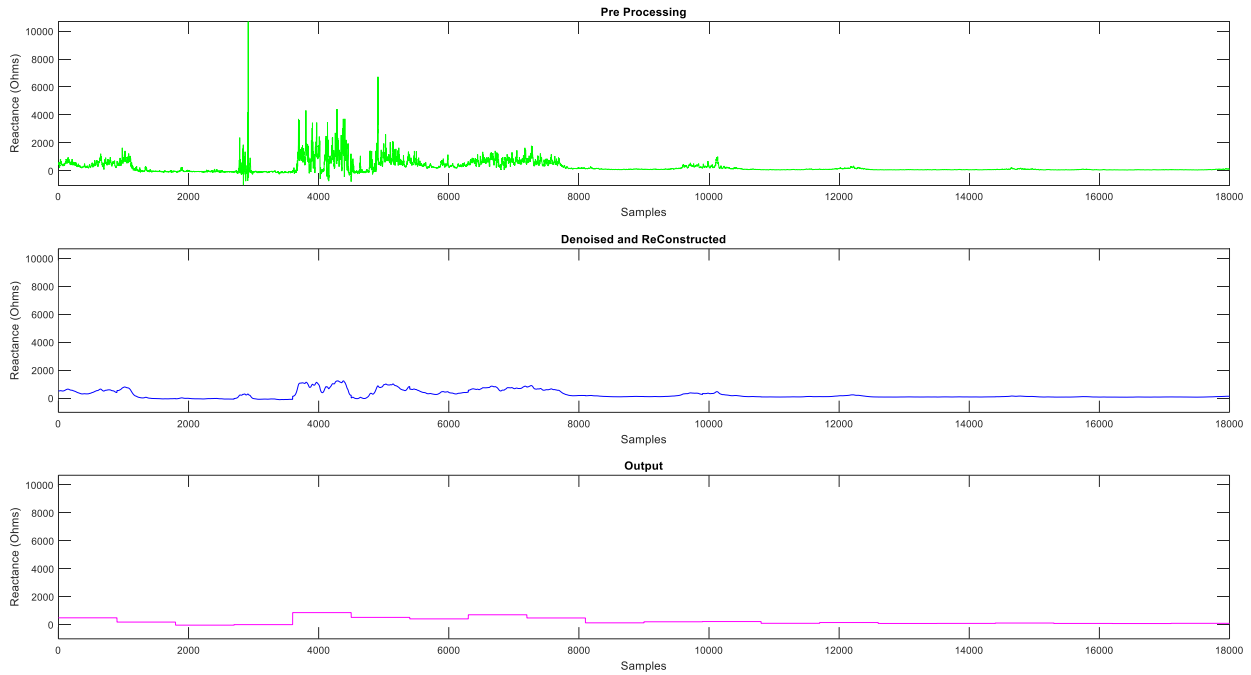
Figure 29. Ten Minute Example 2

This output is a good example of the function of the denoiser and the outlier elimination technique. As can be observed, the process does a good job of removing the large outlier and smoothening the output.

This next extraction is from around 1 a.m. on the 20th of December 2013.

Figure 30. Ten Minute Example 3

Again, the denoiser does a good job and the output produced is very regular. However, the sudden

shift in reactance close to the end is quickly picked up and displayed in the output.

CHAPTER 7

CONCLUSION

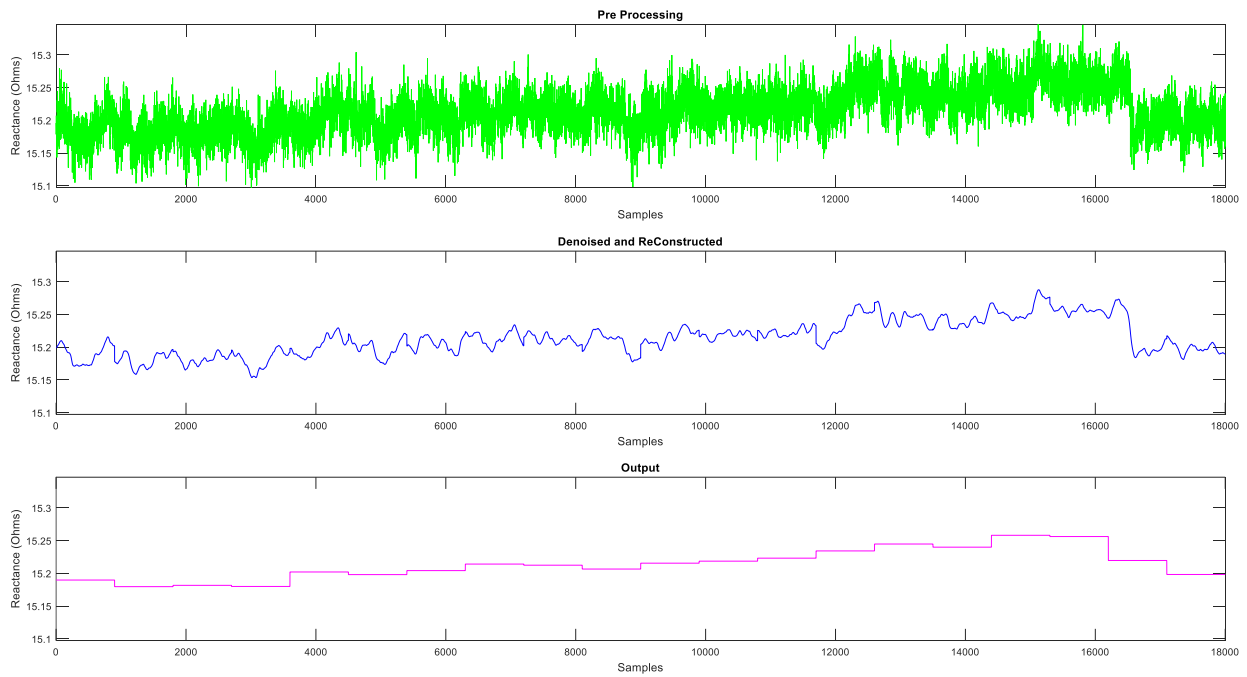The objective of this study was to develop a methodology that can be applied to PMU data in real time to obtain parameters that are not reported. For this study, the reactance of a line was obtained although the process can be easily adapted for resistance as well as other parameters. The methodology developed is not demanding on the processor and also does not require a large quantity of stored data in order to accurately estimate the reactance. Therefore, this method can be implemented to provide near real time updates regarding line parameters.

The developed model was tested using real PMU data and the optimal calculation parameters were found. These parameters were then used to simulate the real time operation of the methodology using the stored data. The simulation showcased how the methodology is robust and is able to perform under varying system conditions throughout the year. The process was able to accurately follow varying trends in the system and provide updates on sudden shifts of the parameter. At the same time, it was able to eliminate outliers and other noisy conditions.

Overall, the proposed methodology is able to perform well and provide accurate estimates of line parameters even with very noisy data and is able to do so while using very little computing resources relative to most other estimation techniques in the literature.

CHAPTER 8

FUTURE WORK

While there exists a variety of ways this research can be extended, both to increase the effectiveness as well as to aid in other applications, two additions that could be great value and interest are discussed below.

In the current methodology, the search for outlier data is quite functional. However, upon finding an outlier data point, the process just replaces it with either the maximum or the minimum limit for that period. This part of the process can be greatly improved by incorporating a prediction algorithm such as Hidden Markov Modeling (HMM) that will look several steps into the past as well as the future in order to provide an accurate prediction for the data point to be filled in.

One notable observation in this study was the correlation between the change in the system frequency and the resulting change in the reactance observed. If this correlation is modeled, the model can be used with minimum mean square estimation to make better estimations of the reactance value by using the reported frequency as well as the rate of change of frequency data.

REFERENCES

REFERENCES

[1] Y. Du and Y. Liao, "Online Estimation of Power Transmission Line," in *North American Power Symposium (NAPS)*, Boston, MA, 2011.

[2] "IEEE Standard for Synchrophasor Data Transfer for Power Systems," 2011.

[3] D. Shi, D. J. Tylavsky, N. Logic and K. M. Koellner, "Identification of Short Transmission-Line Parameters from Synchrophasor Measurements," in *North American Power Symposium*, Calgary, AB, 2008.

[4] X. Wang, H. Sun, B. Zhang, W. Wu and Q. Guo, "Real-Time Local Voltage Stability Monitoring," in *Innovative Smart Grid Technologies - Asia*, Tianjin, 2012.

[5] R. E. Wilson, G. A. Zevenbergen, D. L. Mah and A. J. Murphy, "Calculation of Transmission Line Parameters From Synchronized Measurements," *Electric machines and power systems,* vol. 27, no. 12, pp. 1269-1278, 1999.

[6] C. P. Steinmetz, "Complex quantities and their use in electrical engineering," in *Proceedings of the International Electrical Congress*, Chicago, 1893.

[7] A. G. Phadke , J. S. Thorp and M. G. Adamiak, "A New Measurement Technique for Tracking Voltage Phasors, Local System Frequency, and Rate of Change of Frequency," *IEEE Transactions on Power Apparatus and Systems,* vol. 102, no. 5, pp. 1025-1038, 1983.

[8] A. G. Phadke and J. S. Thorp, Synchronized Phasir Measurements and Their Applications, New York: Springer Science+Business Media, LLC, 2008.

[9] P. Bonanomi, "Phase Angle Measurements with Synchronized Clocks-Principle and Applications," *IEEE Transactions on Power Apparatus and Systems,* vol. 100, no. 12, pp. 5036-5043, 1981.

[10] G. Missout, "Measurement of Bus Voltage Angle Between Montreal and SEPT-ILES," *IEEE Transactions on Power Apparatus and Systems,* vol. 99, no. 2, pp. 536-539, 1980.

[11] G. Missout, J. Beland and G. Bedard, "Dynamic Measurement of the Absolute Voltage Angle on Long Transmission Lines," *IEEE Transactions on Power Apparatus and Systems,* vol. 100, no. 11, pp. 4428-4434, 1981.

[12] U. D. o. Energy, "SGIG Program Progress Report II," 2013.

[13] J. S. Thorp, A. G. Phadke, S. H. Horowitz and M. M. Begovic, "Some applications of phasor measurements to adaptive protection," *IEEE Transactions on Power Systems,* vol. 3, no. 2, pp. 791-798, 1988.

[14] M. J. B. Reddy, D. V. Rajesh, P. Gopakumar and D. K. Mohanta, "Smart Fault Location for Smart Grid Operation Using RTUs and Computational Intelligence Techniques," *IEEE Systems Journal,* vol. 8, no. 4, pp. 1260-1271, 2014.

[15] A. K. Srivastava, "Phasor Measurement (Estimation) Units," Washington State University, Pullman, WA, 2014.

[16] E. M. Stewart, S. Kiliccote, C. McParland and C. Roberts, "Using Micro-Synchrophasor Data for Advanced Distribution Grid Planning and Operations Analysis," Ernest Orlando Lawrence Berkeley National Laboratory, Berkeley, CA, 2014.

[17] "Real-Time Application of Synchrophasors for Improving Reliability," North American Electric Reliability Corporation, Princeton, NJ, 2010.

[18] O. Alsac, N. Vempati, B. Stott and A. Monticelli, "Generalized state estimation [power systems]," in *International Conference on Power Industry Computer Applications* , Columbus, OH, 1997.

[19] C. Borda, A. Olarte and H. Diaz, "PMU-based Line and Transformer Parameter Estimation," in *Power Systems Conference and Exposition*, Seattle, WA, 2009.

[20] G. Valverde, D. Cai, J. Fitch and V. Terzija, "Enhanced State Estimation with Real-time Updated Network Parameters Using SMT," in *Power & Energy Society General Meeting*, Calgary, AB, 2009.

[21] R. Baltensperger, A. Loosli, H. Sauvain, M. Zima, G. Andersson and R. Nuqui, "An implementation of two-stage hybrid state estimation with limited number of PMU," in *International Conference on Developments in Power System Protection* , Manchester, 2010.

[22] R. Matica, V. Kirincic, S. Skok and A. Marusic, "Transmission line impedance estimation based on PMU measurements," in *EUROCON*, Zagreb, 2013.

[23] R. Rubesa, V. Kirincic and S. Skok, "Transmission line positive sequence impedance estimation based on multiple scans of Phasor Measurements," in *IEEE International Energy Conference*, Cavtat, 2014.

[24] S. M. Westervelt, "Transmission Line Positive Sequence Parameter Determination using Synchronized Phasor Measurement," Wichita State University, Wichita, KS, 2015.

[25] A. Back, Theory, Algorithms, and Applications with MATLAB, Philadelphia, PA: Mathematical Optimization Society and the Society for Industrial and Applied Mathematics, 2014.